J|A|C|S
ARTICLES
Published on Web 10/23/2004

Kinetics of Radical Heterolysis Reactions Forming Alkene Radical Cations

John H. Horner,* Laurent Bagnol, and Martin Newcomb*

Contribution from the Department of Chemistry, University of Illinois at Chicago, 845 West Taylor Street, Chicago, Illinois 60607

Received July 1, 2004; E-mail: men@uic.edu

Abstract: Rate constants for heterolytic fragmentation of β-(ester)alkyl radicals were determined by a combination of direct laser flash photolysis studies and indirect kinetic studies. The 1,1-dimethyl-2-mesyloxyhexyl radical (**4a**) fragments in acetonitrile at ambient temperature with a rate constant of $k_{het} > 5 \times 10^9$ s^{-1} to give the radical cation from 2-methyl-2-heptene (**6**), which reacts with acetonitrile with a pseudo-first-order rate constant of $k = 1 \times 10^6$ s^{-1} and is trapped by methanol in acetonitrile in a reversible reaction. The 1,1-dimethyl-2-(diphenylphosphatoxy)hexyl radical (**4b**) heterolyzes in acetonitrile to give radical cation **6** in an ion pair with a rate constant of $k_{het} = 4 \times 10^6$ s^{-1}, and the ion pair collapses with a rate constant of $k \leq 1 \times 10^9$ s^{-1}. Rate constants for heterolysis of the 1,1-dimethyl-2-(2,2-diphenylcyclopropyl)-2-(diphenylphosphatoxy)ethyl radical (**5a**) and the 1,1-dimethyl-2-(2,2-diphenylcyclopropyl)-2-(trifluoroacetoxy)ethyl radical (**5b**) were measured in various solvents, and an Arrhenius function for reaction of **5a** in THF was determined (log $k = 11.16 - 5.39/2.3RT$ in kcal/mol). The cyclopropyl reporter group imparts a 35-fold acceleration in the rate of heterolysis of **5a** in comparison to **4b**. The combined results were used to generate a predictive scale for heterolysis reactions of alkyl radicals containing β-mesyloxy, β-diphenylphosphatoxy, and β-trifluoroacetoxy groups as a function of solvent polarity as determined on the $E_T(30)$ solvent polarity scale.

β-(Ester)alkyl radicals react in rearrangement, substitution, and elimination reactions that are analogous to reactions of closed-shell molecules, although considerably more facile.[1,2] During the past decade, studies by several groups reduced the viable mechanisms for these reactions to two basic types: concerted reactions and reactions involving heterolytic fragmentations that gave transient radical cations.[1] The consensus view in recent years has moved toward heterolytic fragmentation reactions, especially in cases where the putative radical cation intermediate is stabilized as in a styrene radical cation or an enol ether radical cation. For β-(ester)alkyl radicals lacking the stabilizing groups, the mechanistic picture is less clear. Nonetheless, Crich and co-workers have developed synthetic methods employing β-(phosphatoxy)alkyl radicals with the premise that alkene radical cations are formed in ion pairs, and their results, especially in studies of stereoselectivity,[3,4] support the fragmentation mechanism.

For β-(ester)alkyl radicals that heterolyze to give styrene radical cations and enol ether radical cations, laser flash photolysis (LFP) studies have provided valuable mechanistic insights. We report here a combination of direct LFP and indirect kinetic studies of heterolytic fragmentation reactions of β-(ester)-alkyl radicals that give simple alkene radical cations. High reactivity toward heterolysis was achieved by using β-mesyloxy-, β-(diphenylphosphatoxy)-, and β-(trifluoroacetoxy)alkyl radicals and by employing a "reporter group" moiety that rapidly diverts the radical cation intermediate and prevents ion pair recombination. Kinetic studies of β-mesyloxy- and β-phosphatoxyalkyl radical heterolysis reactions in water were reported previously,[5] although, in principle, those reactions could have involved concerted eliminations.[6] Our results provide a predictive kinetic scale for alkyl radical heterolysis reactions in various organic solvents. They provide no support for concerted reaction pathways and, thus, imply that heterolysis reactions giving radical cations are the predominant pathways for all β-(ester)-alkyl radical reactions.

Results and Discussion

We describe the transients formed in radical heterolysis reactions in terms of the ion pair model developed for heterolysis reactions of closed-shell molecules[7] and the analogous radical ion pair model for transients formed by photoinduced electron-transfer (PET) reactions.[8,9] The initial radical heterolysis reaction gives a contact ion pair (CIP) comprised of a radical cation and an anion (Scheme 1). The CIP can collapse to the original radical

(1) Beckwith, A. L. J.; Crich, D.; Duggan, P. J.; Yao, Q. W. *Chem. Rev.* **1997**, *97*, 3273−3312.
(2) Crich, D. In *Radicals in Organic Synthesis*; Renaud, P., Sibi, M. P., Eds.; Wiley-VCH: Weinheim, 2001; Vol. 2, pp 188−206.
(3) Crich, D.; Ranganathan, K. *J. Am. Chem. Soc.* **2002**, *124*, 12422−12423.
(4) Crich, D.; Shirai, M.; Rumthao, S. *Org. Lett.* **2003**, *5*, 3767−3769.
(5) Koltzenburg, G.; Behrens, G.; Schulte-Frohlinde, D. *J. Am. Chem. Soc.* **1982**, *104*, 7311−7312.
(6) Zipse, H. *Acc. Chem. Res.* **1999**, *32*, 571−578.
(7) Winstein, S.; Clippinger, E.; Fainberg, A. H.; Robinson, G. C. *J. Am. Chem. Soc.* **1954**, *76*, 2597−2598.
(8) Gould, I. R.; Farid, S. *Acc. Chem. Res.* **1996**, *29*, 522−528.
(9) Yabe, T.; Kochi, J. K. *J. Am. Chem. Soc.* **1992**, *114*, 4491−4500.

Scheme 1

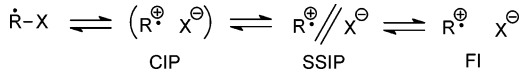

Scheme 2

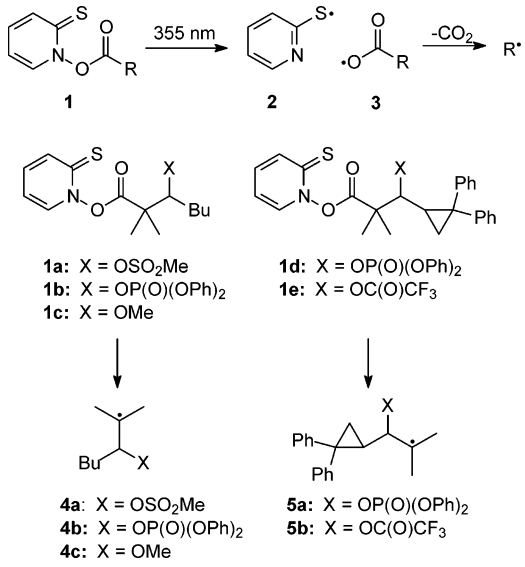

or to a rearranged radical, or it can solvate to give a solvent-separated ion pair (SSIP). In turn, the SSIP can return to the CIP or further solvate to give diffusively free ions (FI). Nucleophiles, bases, and reducing agents might react with radical cations at any stage in the sequence.

The β-(ester)alkyl radical precursors used in this work were PTOC esters[10] **1** (Scheme 2), which were prepared from the corresponding carboxylic acids by conventional methods. Synthetic details for the precursors are given in the Supporting Information. Laser photolysis (355 nm) of PTOC esters in He-sparged flowing solutions cleaved the weak N−O bond to give the pyridine-2-thiyl radical (**2**) and an acyloxyl radical (**3**) that decarboxylated rapidly (subnanosecond) to give the desired radical (Scheme 2). Byproduct radical **2** has a long-wavelength absorbance with $\lambda_{max} = 490$ nm,[11] and the initial absorbance from **2** can be used to estimate yields from radical reactions in some cases. Radical **2** appears to decay mainly by self-coupling in a diffusion-controlled process. PTOC esters **1** also were used as precursors in preparative reactions. The reactions were initiated by visible-light photolysis, which cleaves the PTOC esters, the chain sequence was propagated by reactions of transients with a thiol, and thiyl radicals reacted with another molecule of PTOC ester to continue the chain reaction.

Precursors **1a**−**1c** gave the series of alkyl radicals **4** that was studied in LFP and preparative reactions. The radicals contain an excellent β-mesylate leaving group (**4a**), a good β-phosphate leaving group (**4b**), and a poor β-methoxide leaving group (**4c**). Radical **4c** was expected not to heterolyze and served as a blank system for spectroscopy. Precursors **1d** and **1e** gave radicals **5** containing β-phosphate and β-trifluoroacetate leaving groups and a reporter-group[12] moiety for direct detection in LFP studies.

(10) The acronym PTOC is for pyridine-2-thioneoxycarbonyl. PTOC esters were originally developed by Barton's group and are also known as Barton esters. See: Barton, D. H. R.; Crich, D.; Motherwell, W. B. *Tetrahedron* **1985**, *41*, 3901−3924.
(11) Alam, M. M.; Watanabe, A.; Ito, O. *J. Org. Chem.* **1995**, *60*, 3440−3444.
(12) Newcomb, M.; Tanaka, N.; Bouvier, A.; Tronche, C.; Horner, J. H.; Musa, O. M.; Martinez, F. N. *J. Am. Chem. Soc.* **1996**, *118*, 8505−8506.

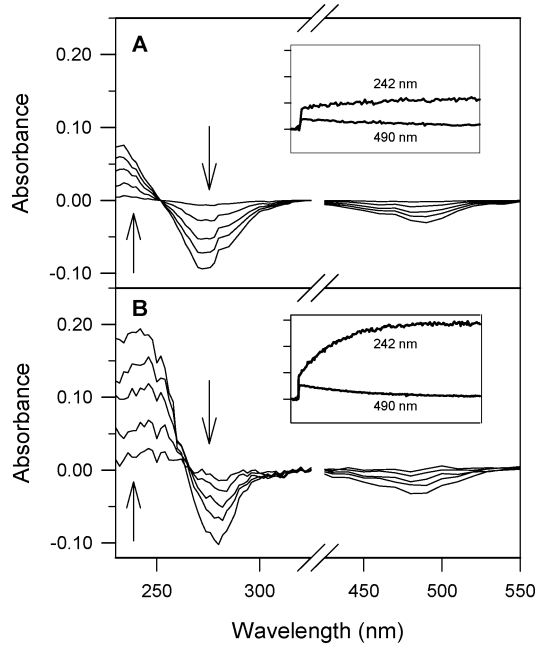

Figure 1. Time-resolved spectra from reactions of radicals **4c** (A) and **4a** (B) in acetonitrile over ca. 14 and 2.5 μs, respectively. The spectra are baseline corrected by subtraction of an early time trace; growing peaks have positive absorbances, whereas decaying peaks have negative absorbances. The insets show the kinetic traces at 490 nm (from decay of radical **2**) and at 242 nm for the first 4 μs of the reactions.

Mesylate Heterolysis and Radical Cation Trapping. Figure 1A shows the time-resolved spectral behavior when radical **4c** was produced in acetonitrile. A relatively small signal with $\lambda_{max} \approx 234$ nm grew in with a rate constant equal to those for decay of the signals that have $\lambda_{max} = 278$ nm and $\lambda_{max} = 490$ nm. The 490 nm signal is known to arise from radical **2**,[11] and we assign the decaying signal at 278 nm to radical **2** also. The growing signal at 234 nm is due to 2,2′-dipyridyl disulfide, formed by self-coupling of radical **2**, and this assignment is consistent with the UV-spectrum of 2,2′-dipyridyl disulfide, which has λ_{max} at 236 nm. Note that there is no indication of a UV spectrum that can be attributed to radical **4c**.

LFP production of radical **4a** in acetonitrile was followed by growth of a strong signal with $\lambda_{max} = 242$ nm in addition to signal decay at $\lambda_{max} = 278$ nm and at $\lambda_{max} = 490$ nm (Figure 1B). The 242 nm signal grew in faster than the other signals decayed, indicating the presence of a new transient. Limited previous studies[13,14] reported that alkene radical cations have weak UV−visible absorbances, but several lines of evidence indicate that the spectrum observed here was not from alkene radical cation **6**. Trapping studies showed that radical **4a** could not be trapped by PhSH (see below), which requires that the rate of heterolysis of radical **4a** was more than 3 orders of magnitude faster than signal growth at 242 nm. The 242 nm signal was essentially completely suppressed by 1×10^{-3} M diisopropylethylamine in CH_3CN, consistent with diffusion-controlled reaction with (undetectable) radical cation **6** before it could react to give the species absorbing at 242 nm. In addition, the 242 nm signal was persistent in acetonitrile, even in the presence of high concentrations of methanol (see below).

(13) Mehnert, R.; Brede, O.; Cserep, G. *Radiat. Phys. Chem.* **1985**, *26*, 353−363.
(14) Clark, T.; Teasley, M. F.; Nelsen, S. F.; Wynberg, H. *J. Am. Chem. Soc.* **1987**, *109*, 5719−5724.

Scheme 3

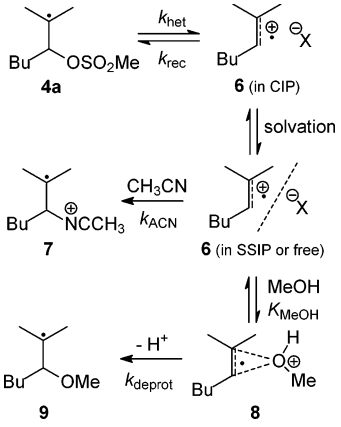

The spectrum also cannot result from the mesylate anion formed by heterolysis, which has no major absorbance at wavelengths longer than 220 nm. Alkene radical cations are known to react with acetonitrile,[15] and we ascribe the new signal to distonic radical cations **7** formed by the addition of acetonitrile to radical cation **6** (Scheme 3). Thus, radical cation **6** apparently absorbed too weakly to be detected, but adduct **7** could be observed. Note that we show one isomer for radical cation **7** in the scheme, but two isomers are expected from trapping at C2 and C3 of **6**; DFT calculations indicate that the tertiary radical **7** shown in the scheme will be about 3 kcal/mol more stable than the isomeric secondary radical.[16]

The rate constant for formation of product **7** was relatively insensitive to solvent polarity. A series of reactions of radical **4a** in acetonitrile containing increasing amounts of 2,2,2-trifluoroethanol (TFE) was performed, and the rate constant for formation of **7** increased only slightly from $k = 1 \times 10^6\ s^{-1}$ in neat acetonitrile to $k = 2 \times 10^6\ s^{-1}$ in a solution of acetonitrile containing 5% TFE, which is high in polarity as evaluated by its $E_T(30)$ solvent polarity parameter.[17] The modest solvent polarity effect is different than the effects found in heterolysis reactions of radicals that give styrene and enol ether radical cations,[18−20] and more dramatic solvent polarity effects also were found in studies of radicals **5** discussed below, where the rate-limiting step is the initial radical heterolysis reaction. The small solvent effect is consistent with the proposal that the rate-limiting step was the reaction of radical cation **6** with acetonitrile, that is, $k_{ACN} = 1 \times 10^6\ s^{-1}$. As a corollary, equilibria involving radical cation **6** and radical **4a** or ion pairs containing the radical cation apparently were only slightly perturbed by changes in solvent polarity.

The interpretation of the results with **4a** was supported by a series of LFP studies in which methanol was added to the reaction mixtures. In these reactions, the intensity of the signal at 242 nm was reduced as the concentration of MeOH increased (Figure 2A), indicating the formation of a methanol-trapping product, and the formation of methanol-trapped products was

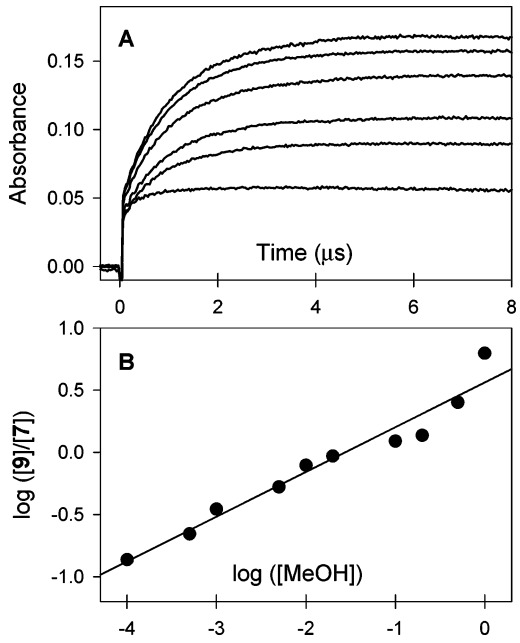

Figure 2. (A) Kinetic traces at 242 nm for reactions of **4a** in acetonitrile containing (from the top) 0, 0.0001, 0.001, 0.01, 0.1, and 1.0 M MeOH. (B) Ratio of products in methanol competition experiments versus methanol concentration; the values for the regression line are discussed in the text.

confirmed in preparative reactions. When radical **4a** was generated in the presence of MeOH and *tert*-butyl mercaptan, 2-methyl-2-methoxyheptane and 2-methyl-3-methoxyheptane were formed in 90% yield and a 1:3.5 ratio (2-MeO:3-MeO).

At the qualitative level, the methanol results indicate that MeOH intercepted radical cation **6** in competition with acetonitrile trapping. Importantly, the signal at 242 nm that did form in the presence of methanol was relatively persistent, decaying on the millisecond time scale at a rate similar to that for decay in the absence of methanol. This demonstrates that the transient giving rise to the 242 nm signal cannot be radical cation **6**, which should react relatively rapidly with methanol.

At the quantitative level, the methanol-trapping results were complex. The rate constant for signal formation at 242 nm was not significantly altered when methanol was present, even when the amount of signal formed was considerably reduced. This kinetic behavior requires that the methanol reaction involved the formation of another transient in equilibrium with radical cation **6** and that the new transient gave products in a rate-limiting reaction that has a rate constant comparable to that for reaction of **6** with acetontirile.[21] We propose that adduct **8** is produced in a fast equilibrium reaction, and deprotonation of **8** to give methoxy-substituted radical **9** is the rate-limiting step (Scheme 3). We show one product from the methanol-trapping reaction, but both the secondary and the tertiary alcohol products were formed in preparative reactions. This model is the same as that deduced by Arnold and co-workers for reactions of alkene radical cations with MeOH in acetonitrile solution,[15] and it is consistent with expectations that the loss of neutral MeOH from intermediate **8** will be an exceedingly fast reaction.

(15) Mangion, D.; Arnold, D. R. *Acc. Chem. Res.* **2002**, *35*, 297−304.
(16) See Supporting Information.
(17) Reichardt, C. *Chem. Rev.* **1994**, *94*, 2319−2358.
(18) Choi, S. Y.; Crich, D.; Horner, J. H.; Huang, X. H.; Martinez, F. N.; Newcomb, M.; Wink, D. J.; Yao, Q. W. *J. Am. Chem. Soc.* **1998**, *120*, 211−212.
(19) Choi, S. Y.; Crich, D.; Horner, J. H.; Huang, X. H.; Newcomb, M.; Whitted, P. O. *Tetrahedron* **1999**, *55*, 3317−3326.
(20) Horner, J. H.; Taxil, E.; Newcomb, M. *J. Am. Chem. Soc.* **2002**, *124*, 5402−5410.

(21) If reactions of radical cation **6** involved a simple competition between acetonitrile and MeOH trapping, then the observed rate constant for formation of **7**, which equals that for decay of **6**, must increase as a function of MeOH concentration. For example, if 75% of **6** was trapped by MeOH, then the observed rate constant would be 4 times that found in the absence of MeOH. In practice, the observed rate constant was essentially unchanged when the signal at 242 nm was decreased by more than 75%.

The methanol concentration effect on the intensity of the 242 nm signal clearly was not linear. As shown in Figure 2A, the 242 nm signal growth was noticeably decreased at concentrations of MeOH as low as 1×10^{-4} M, but it was not completely suppressed by 0.1 M MeOH. This behavior is consistent with aggregation of methanol in acetonitrile in a relatively unreactive form; presumably, the nucleophilicity of hydrogen-bonded MeOH is reduced considerably from that of monomeric MeOH in acetonitrile. In such a case, the ratio of products **9** and **7** would be described by eq 1, where the rate constants are those labeled in Scheme 3, the value K_{MeOH} is a composite of the equilibrium constant for formation of the methanol adduct and the dissociation constant(s) for aggregated MeOH, and X is the effective aggregation number for MeOH. Equation 2 is the logarithmic form of eq 1.

$$[\mathbf{9}]/[\mathbf{7}] = k_{deprot}K_{MeOH}[MeOH]^{1/X}(k_{ACN})^{-1} \quad (1)$$

$$\log([\mathbf{9}]/[\mathbf{7}]) = \log(K_{MeOH}k_{deprot}/k_{ACN}) + 1/X \log([MeOH]) \quad (2)$$

Using the model of Scheme 3, we calculated the relative amount of adducts **7** formed for each reaction from the observed intensity of the 242 nm signal and assigned the remainder to products **9**. Figure 2B is a plot of the log of the product ratio as a function of the log of MeOH concentration (e.g., eq 2). The linearity of the plot over a 4 orders of magnitude change in MeOH concentration is noteworthy. The slope is 0.36 ± 0.03, indicating that the effective aggregation number for MeOH in acetonitrile was about 3. The intercept of the plot is 0.56 ± 0.06, which is the logarithm of the composite of the rate constants and K_{MeOH}. Because the observed rate for formation of the 242 nm signal was relatively constant when MeOH was present, $k_{deprot} \approx k_{ACN}$, in which case $K_{MeOH} \approx 3.6\ M^{-1}$, where K_{MeOH} is a combination of the equilibrium constant for complex formation and dissociation constant(s) for aggregated MeOH.[22]

As noted above, reversible complexation of alkene radical cations with methanol in acetonitrile solvent was previously deduced by Arnold and co-workers from the products formed in photochemical NOCAS (nucleophile-olefin combination, aromatic substitution) reactions that involve alkene radical cation intermediates.[15] Reversible adduct formation as shown in Scheme 3 also is consistent with stereoselectivity studies by Crich and co-workers who observed racemization in cyclization of an alkene radical cation from a chiral precursor containing a hydroxy group, whereas the analogous amine-containing radical cation cyclized stereoselectively.[4] Reactions of MeOH with styrene radical cations[23] and with enol ether radical cations[20] were reported to be second-order processes with rate constants on the order of $10^6-10^7\ M^{-1}\ s^{-1}$, but it is possible that the nonlinear concentration effect of MeOH was not apparent in these studies due to a limited range of MeOH concentrations studied.

Reactions of radical **4a** in acetonitrile or THF in the presence of thiophenol confirmed that the heterolysis reaction giving radical cation **6** was quite rapid. Thiophenol reacts with alkyl radicals by H-atom transfer with $k \approx 1 \times 10^8\ M^{-1}\ s^{-1}$,[24,25] but the only product (>98%) found in preparative reactions of radical **4a** in the presence of up to 1 M PhSH was 2-methyl-2-heptene, apparently formed by reduction of radical cation **6** by PhSH.[26,27] The absence of the H-atom trapping product 2-methyl-3-mesyloxyheptane, which was demonstrated to be stable to the reaction conditions, establishes a lower limit for the rate constant for the heterolysis reaction of **4a** of $k_{het} > 5 \times 10^9\ s^{-1}$. It also suggests that collapse of the CIP to return radical **4a** was slower than (presumably) diffusion-controlled reduction of **6** by PhSH and/or that the equilibrium for the heterolysis reaction favored the CIP.

The accumulated results with β-mesylate radical **4a** show that heterolysis in CH_3CN to give radical cation **6** is exceedingly fast, with a subnanosecond lifetime for **4a**. Fast heterolysis reactions of α-methoxy-β-mesylate,[28] α-aryl-β-mesylate,[29] and β-aryl-β-mesylate[30] radicals in organic solvents were previously reported, but these radicals were precursors to stabilized enol ether and styrene radical cations. In pulse radiolysis studies in water,[5] the rate constant reported for reaction of the radical from propyl mesylate was $2 \times 10^5\ s^{-1}$, whereas the rate constants for reactions of the radicals from butyl mesylate and isobutyl mesylate were $>10^6\ s^{-1}$, which reflected the kinetic limit of the method.[5] It appears that the rate constant reported for heterolysis of the radical from propyl mesylate is anomalous.

The limiting value for the rate constant for heterolysis of **4a**, $k_{het} > 5 \times 10^9\ s^{-1}$, suggests that the equilibrium reaction for forming the CIP in CH_3CN is exergonic in acetonitrile. That conclusion is based on the assumption that the upper limit for the rate constant for collapse of the CIP is $k_{rec} < 4 \times 10^9\ s^{-1}$, which is the rate constant for the highly exothermic collapse in acetonitrile of the CIP comprised of the diphenylmethyl cation and the chloride anion.[31] In the latter case, the rate of CIP collapse is controlled by the energy required to reorganize the acetonitrile solvent; that is, the reaction occurs in the so-called "solvent polarization caging regime".[31] If the equilibrium between radical **4a** and its CIP in acetonitrile favors the CIP, then accumulation of diffusively free ions is expected because

(22) Consistent with this model, MeOD suppressed the 242 nm signal less than MeOH when similar concentrations were compared. For example, at 0.1 M MeOD, the 242 nm signal was reduced by 30%, whereas the signal was reduced by 55% with 0.1 M MeOH. Isotope effects are expected both in the aggregation of MeOD (stronger hydrogen-bonding interactions) and in the rate of deprotonation of intermediate **8** (slower deprotonation), and the two isotope effects should work in concert to reduce production of the product radical **9**.

(23) Johnston, L. J.; Schepp, N. P. *J. Am. Chem. Soc.* **1993**, *115*, 6564−6571.

(24) Franz, J. A.; Bushaw, B. A.; Alnajjar, M. S. *J. Am. Chem. Soc.* **1989**, *111*, 268−275.

(25) Newcomb, M.; Choi, S. Y.; Horner, J. H. *J. Org. Chem.* **1999**, *64*, 1225−1231.

(26) Reaction of PhSH with enol ether radical cations (presumed to occur by electron transfer) to give enol ether products was previously shown to be faster than reactions of the enol ether radical cations with aqueous solvent. See: Giese, B.; Burger, J.; Kang, T. W.; Kesselheim, C.; Wittmer, T. *J. Am. Chem. Soc.* **1992**, *114*, 7322−7324. Giese, B.; Beyrich-Graf, X.; Burger, J.; Kesselheim, C.; Senn, M.; Schafer, T. *Angew. Chem., Int. Ed. Engl.* **1993**, *32*, 1742−1743.

(27) A referee noted that the reduction of radical cation **6** by PhSH could be an inner-sphere process involving nucleophilic capture of the radical cation by PhSH, deprotonation of the adduct to give the β-phenylthio radical, and elimination of phenylthiyl radical to give the observed alkene product. The distinction between an outer-sphere and an inner-sphere reduction of the alkene radical cation is not critical for the studies reported here, but ancillary studies appear to support an outer-sphere process. Specifically, substitution of thioanisole for thiophenol in matched reactions resulted in only a ca. 20% decrease in the amount of alkene **11** formed in the reaction, and reaction of radical **4a** with MeOH in the presence of *t*-BuSH gave ca. 90% yield of methyl ethers from methanol trapping. For the latter case, *t*-BuSH would be expected to be a better nucleophile than PhSH.

(28) Taxil, E.; Bagnol, L.; Horner, J. H.; Newcomb, M. *Org. Lett.* **2003**, *5*, 827−830.

(29) Lancelot, S. F.; Cozens, F. L.; Schepp, N. P. *Org. Biomol. Chem.* **2003**, *1*, 1972−1979.

(30) Bagnol, L.; Horner, J. H.; Newcomb, M. *Org. Lett.* **2003**, *5*, 5055−5058.

(31) Peters, K. S.; Li, B. L. *J. Phys. Chem.* **1994**, *98*, 401−403.

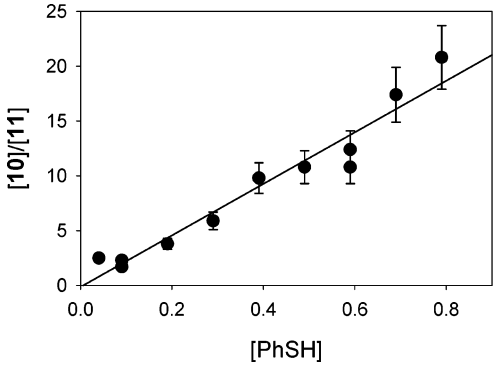

Figure 3. Ratios of phosphate **10** to alkene **11** observed in reactions of 0.02 M PTOC ester **1b** with PhSH in CD_3CN.

Scheme 4

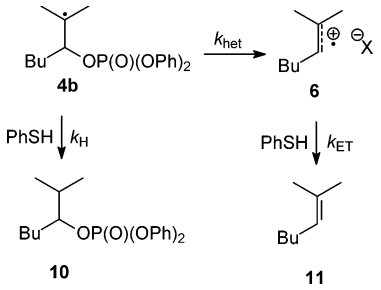

solvation of the CIP in acetonitrile and diffusive escape from the SSIP will have rate constants in the range of $(2-30) \times 10^8$ s^{-1},[8,20,31] which are comparable to the expected CIP collapse rate constant.

Phosphate Heterolysis. LFP generation of β-phosphate radical **4b** in acetonitrile gave time-resolved spectra similar to those obtained with methoxy radical **4c**. The growth of signal at $\lambda = 242$ nm (5×10^5 s^{-1}) was somewhat faster than signal decay at $\lambda = 278$ nm (3×10^5 s^{-1}), but the intensity of the 242 nm signal growth relative to the 278 nm signal decay was comparable to that observed with **4c**. Thus, the LFP results indicate that adduct **7** was not formed in appreciable amounts.

Preparative reactions of **4b** in the presence of thiophenol, however, demonstrated that the heterolysis reaction giving radical cation **6** in an ion pair was relatively fast and permitted an estimation of the rate constant for heterolysis. In a series of reactions, radical **4b** was produced in the presence of varying concentrations of PhSH in acetonitrile-d_3, and the products were analyzed by NMR spectroscopy. Both 3-(diphenylphosphatoxy)-2-methylheptane (**10**) and 2-methyl-2-heptene (**11**) were formed in these reactions. The alkane phosphate product **10** was formed by H-atom trapping of radical **4b** by PhSH, and alkene **11** was formed by reduction of radical cation **6** by PhSH (Scheme 4).[26,27] The ratio [**10**]/[**11**] is plotted against the concentration of PhSH in Figure 3. Note that the ratios have relatively large errors due to the small amounts of alkene formed. It is possible that some of alkene **11** was consumed by addition of PhSH, but we did not observe thiophenol addition products.

The slope of the plot in Figure 3 is 23 ± 4 M^{-1} (error at 2σ). The slope is equal to k_H/k_{het}, and, by using a rate constant for reaction of radical **4b** with PhSH[24,25] of 1×10^8 M^{-1} s^{-1}, one obtains a rate constant for heterolysis of **4b** of $k_{het} = 4 \times 10^6$ s^{-1}. The intercept of the plot in Figure 3 is effectively zero, and a zero intercept would result when the heterolysis reaction

Scheme 5

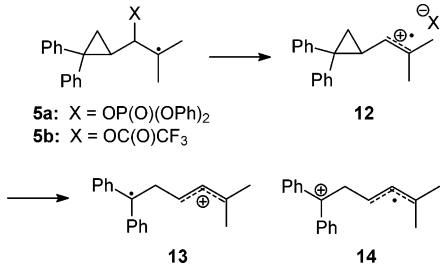

is irreversible under the experimental conditions.[32] Thus, the reduction of the radical cation appears to be faster than CIP collapse when one considers the entire concentration range of PhSH studied. At the low concentrations of PhSH (<0.1 M), however, an apparent curvature in the plot suggests that the collapse reaction was competitive with the radical cation reduction reaction. If one assumes that reduction of radical cation **6** by PhSH is a diffusion-controlled process with a rate constant of $k_{ET} \approx 1 \times 10^{10}$ M^{-1} s^{-1}, one can set a limiting value on the rate constant for CIP recombination $k_{rec} < 1 \times 10^9$ s^{-1}. If the apparent curvature in the plot is real, and the infinite dilution value for the ratio of [**10**]/[**11**] is 2.5, then the rate constant for collapse of the CIP solved from this intercept[32] is $k_{rec} = 1 \times 10^9$ s^{-1} (again assuming a diffusion-controlled reaction between the radical cation and PhSH). The equilibrium population of the CIP from radical **4b** in acetonitrile is small ($\leq$0.4%) in any event. In less polar solvents, the heterolysis will be slower, and the population of the CIP will be smaller.

The PhSH trapping results for **4b** are consistent with the LFP results. The equilibrium constant between radical **4b** and the CIP apparently favors the neutral radical. If the rate constant for escape from the CIP is on the order of 1×10^8 s^{-1}, then the rate of formation of diffusively free radical cation **6** could be about 10% of the rate of heterolysis of **4b**, or ca. 4×10^5 s^{-1}. Radical−radical coupling reactions of **4b** in the LFP experiments will compete with the formation of diffusively free **6**, resulting in limited formation of acetonitrile adduct **7**.[33]

Direct Measurements of Radical Heterolysis Rate Constants. Radicals **5** were produced in LFP studies using PTOC esters **1d** and **1e** as the precursors. Radicals **5** incorporate a diphenylcyclopropane reporting group[12] adjacent to the leaving group, and in related α-methoxy-β-substituted radicals, precursors to enol ether radical cations, the same reporter group was found to promote heterolysis as well as provide a UV-observable product.[34] Heterolysis reactions of radicals **5** will give radical cation **12**, which was expected to rearrange rapidly to distonic radical cations **13** and/or **14** (Scheme 5). The diphenylalkyl radical chromophore in **13** will have an absorbance with $\lambda_{max} \approx 335$ nm, whereas the diphenylalkyl cation chromophore in

(32) Newcomb, M. *Tetrahedron* **1993**, *49*, 1151−1176.
(33) Schulte−Frohlinde and co-workers reported rate constants for the heterolysis of two β-phosphate radicals that gave isobutene radical cation in water of $(1-3) \times 10^4$ s^{-1}.[5] The studies involved pulse radiolysis of aqueous solutions to generate the hydroxyl radical, which abstracted H-atom from the substrate, and time-resolved conductivity measurements. From our results, one would predict that reaction of radical **4b** in water would be much faster, $k \approx 4 \times 10^8$ s^{-1}. The diphenyl phosphate group in **4b** is more reactive than the dialkyl phosphate groups in the earlier study, and a more stable trisubstituted radical cation is formed by heterolysis of **4b**. Possibly most importantly, the rate constant for reaction of **4b** is that for formation of radical cation in an ion pair, whereas the early study measured the rate of acid formation from reaction of the radical cation with water.
(34) Newcomb, M.; Miranda, N. *J. Org. Chem.* **2004**, *69*, 6515−6520.

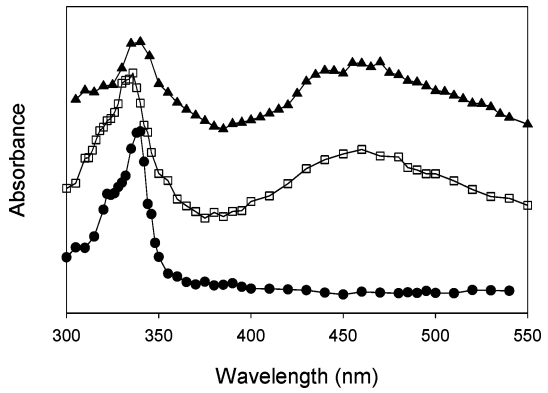

Figure 4. Product spectra from reactions of radical **5a** in TFT (●) and in acetonitrile (□) and from oxidation of alkene **15** by the chloranil triplet in acetonitrile (▲). The spectra were scaled to arbitrary absorbance units and offset for clarity. Note that the spectra from radical **5a** are for the products that form in the reactions; the spectrum of byproduct radical **2** and the initial bleaching effect were subtracted from the experimental spectra.

Scheme 6

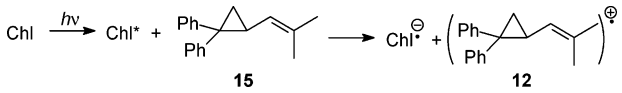

14 was expected to absorb with $\lambda_{max} \approx 450$ nm.[35,36] The 2,2-diphenylcyclopropylcarbinyl radical cleaves with a rate constant of 5×10^{11} s^{-1} at ambient temperature,[37] and ring opening of radical cation **12** was expected to be even faster. Thus, it was anticipated that the ring-opening reporting reaction was likely to compete with reactions of radical cation **12** in an ion pair.

Radicals **5** were studied in a variety of solvents. Figure 4 shows the final product spectrum for reaction of **5a** in trifluoromethylbenzene (trifluorotoluene, TFT), which is typical for the reactions in low polarity solvents. The signal with $\lambda_{max} =$ 334 nm is from distonic radical cation **13** or a product from **13** in which the cation moiety has reacted with solvent. The ultimate signal intensity at $\lambda = 334$ nm was compared to the initial signal intensity at $\lambda = 490$ nm (from byproduct radical **2**) to estimate yields of **13**, which were essentially quantitative for reactions in THF and TFT and ca. 75% for reactions of **5a** in cyclohexane.

In the medium polarity solvent acetonitrile, the signal intensity at $\lambda = 334$ nm from reactions of radicals **5** was reduced, and a new signal with $\lambda_{max} \approx 460$ nm was observed (Figure 4). In the reaction of radical **5b** in CH_3CN at ambient temperature and in reactions of **5a** in CH_3CN at low temperatures, the two signals grew in with comparable rates, suggesting that they arose from a mixture of products **13** and **14**.

The identities of products **13** and **14** were confirmed by oxidation of alkene **15** in acetonitrile by the chloranil triplet (Chl*), a strong oxidant formed by 355 nm photolysis of chloranil (Scheme 6). Triplet chloranil oxidized alkene **15** in a diffusion-controlled reaction, and time-resolved spectra were obtained. For the analysis of these spectra, we subtracted time-resolved spectra obtained when Chl* was produced in the presence of dihydropyran in an otherwise matched reaction. The enol ether and its radical cation have no appreciable absorbance in the UV−visible range studied here, and time-resolved spectra from the enol ether reaction show decay of Chl* and growth of the chloranil radical anion. Subtraction of the spectra from the enol ether oxidation reaction from those obtained in the oxidation of alkene **15** gave difference spectra showing two absorbances from reactions of radical cation **12** (Figure 4) that are similar to those in the spectra obtained from the reaction of radicals **5** in acetonitrile.

Table 1. Rate Constants for Heterolysis Reactions of Radicals **5** at Ambient Temperature[a]

solvent	$E_T(30)$	**5a**	**5b**
cyclohexane	30.9	0.64	
toluene	33.9	7.6	1.5
THF	37.4	17	4.2
TFT[b]	38.5	21	2.7
acetonitrile	45.6	140[c]	43

[a] Observed rate constants at 22 ± 2 °C in units of 10^6 s^{-1}. [b] TFT = trifluorotoluene. [c] The rate constant for reaction of **5a** in acetonitrile at 20 °C was calculated from a measured rate constant of 4.6×10^7 s^{-1} at −20 °C and a log *A* term of 11.16; see text.

Ultrafast ring opening of the reporter group in radical cation **12** was demonstrated by reaction of β-phosphate radical **5a** in the presence of PhSH in acetonitrile. From the LFP results (see below), radical **5a** heterolyzes in acetonitrile at ambient temperature with a rate constant of $k = 1.4 \times 10^8$ s^{-1}. In the preparative reaction with 1 M PhSH, we obtained no detectable amount of alkene **15** from trapping of radical cation **12**. Assuming a conservative limit of 10% for the detection of **15** and diffusion-controlled reduction of alkene radical cation **12** by PhSH, the ring opening of **12** would have a rate constant $k > 1 \times 10^{11}$ s^{-1} at ambient temperature. That limit is larger than the rate constants for dynamic phenomena in ion pairs, including collapse of the CIP in CH_3CN. Therefore, the observed rate constants for reactions of radicals **5** apparently are the rate constants for the initial heterolysis reactions that produce **12** in a CIP. It is possible that reactions of radicals **5** proceeded directly to ring-opened products, that is, reaction by concerted cleavage of the leaving group and a cyclopropane bond, but that would not complicate the kinetic analysis.

The rate constants for heterolysis of radicals **5** in various solvents at ambient temperature are listed in Table 1. In low polarity solvents, product **13** was formed, and a mixture of **13** and **14** was formed in acetonitrile. The rate constant for reaction of radical **5a** in acetonitrile at ambient temperature was greater than the temporal limit of our unit. To determine a value for the reaction at 20 °C, rate constants were measured at low temperatures and used with the log *A* term found for reaction of **5a** in THF (see below) to calculate the rate constant for reaction at ambient temperature.

The heterolysis reaction of radical **5a** in acetonitrile provides data for evaluation of the kinetic effect of the cyclopropane group. Radical **5a** reacted 35 times faster than radical **4b**, and the accelerating effect of the cyclopropane in **5a** is nearly an order of magnitude greater than the acceleration due to the phenyl group in radical **16**, where we take the rearrangement rate constant for isomerization of **16** to its benzylic radical product in acetonitrile ($k_{obs} = 1.8 \times 10^7$ s^{-1})[18,19] to be the rate constant for heterolysis. In fact, radical **5a** reacted faster than radical **17**, which gives the corresponding radical cation with a rate constant of $k_{het} = 8 \times 10^7$ s^{-1} in CH_3CN at ambient

(35) Faria, J. L.; Steenken, S. *J. Phys. Chem.* **1993**, *97*, 1924−1930.
(36) Johnston, L. J. *Chem. Commun.* **1998**, 2411−2424.
(37) Newcomb, M.; Johnson, C. C.; Manek, M. B.; Varick, T. R. *J. Am. Chem. Soc.* **1992**, *114*, 10915−10921.

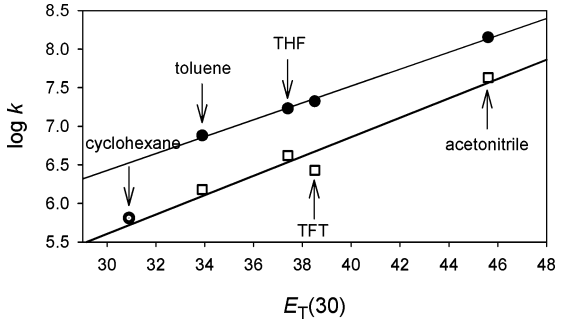

Figure 5. Rate constants for heterolysis reactions of radicals **5a** (●) and **5b** (□) at ambient temperature as a function of solvent polarity. The rate constant for reaction of **5a** in cyclohexane was not included in the regression line.

temperature.[38] The kinetic effect of the cyclopropane in the heterolysis of the radical mirrors the behavior in heterolytic fragmentations of closed-shell molecules, where a cyclopropyl group has a greater accelerating effect than a phenyl group.[39,40]

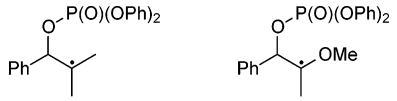

16 **17**

Table 1 also lists the $E_T(30)$ solvent polarity values for the various solvents. The $E_T(30)$ solvatochromic values correlate with many polar reactions,[17] including radical heterolysis reactions,[18,19,30,41] and can be used to estimate solvent polarity effects. Plots of log k versus $E_T(30)$ are shown in Figure 5. For the β-phosphate radical **5a**, the rate constant for reaction in cyclohexane clearly is out of line with the other rate constants, and the reduced yield of **13** from reaction of **5a** in cyclohexane suggests that there were unknown reactions in this solvent. Excluding the cyclohexane rate constant, the slope for the data for **5a** is 0.109 ± 0.004. For the heterolysis of radical **5b**, the regression line has a slope of 0.12 ± 0.02. In heterolysis reactions of β-aryl-β-(ester)alkyl radicals that give styrene radical cation products, plots of log k versus $E_T(30)$ had slopes of 0.109 ± 0.004[30] and 0.128 ± 0.003.[41] The similarity in the values for the different systems suggests a generality in transition-state structures and degrees of polarization for various radical heterolysis reactions.

The heterolysis reaction of radical **5a** in THF was studied over the temperature range from −39 to 51 °C (Figure 6). These data give an Arrhenius function of log $k = (11.16 \pm 0.12) - (5.39 \pm 0.15)/\theta$, where $\theta = 2.3RT$ in kcal/mol, and errors are at 2σ. Limited low-temperature studies (−40 to −4 °C) of **5a** in acetonitrile gave a low-precision Arrhenius function with a similar entropic term: log $k = (11.0 \pm 0.4) - (3.8 \pm 0.4)/\theta$. The entropic terms found here are similar to those found in a number of radical heterolysis reactions that give styrene radical cations and enol ether radical cations.[18−20,30] Although one might anticipate that the fragmentation will be entropy releasing, radical organization in the transition state and solvent reorganization to accommodate charge formation apparently result in negative entropies of activation.

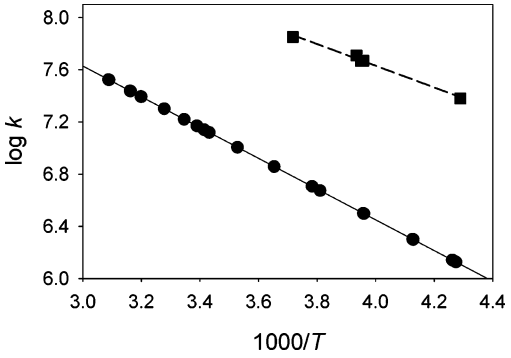

Figure 6. Temperature-dependent plots for heterolysis of radical **5a** in THF (●) and in acetonitrile (■). The regression lines are the Arrhenius functions given in the text.

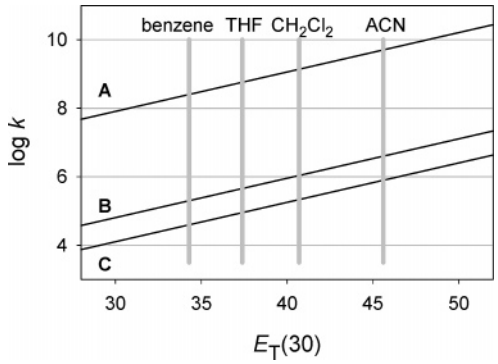

Figure 7. Estimated rate constants at ambient temperature for heterolysis of β-(ester)alkyl radicals that give trisubstituted alkene radical cations: (A) mesylates (lower limit), (B) diphenyl phosphates, (C) trifluoroacetates. The gray bars are the $E_T(30)$ values for common organic solvents (ACN = acetonitrile).

Kinetic Model for Radical Heterolysis Reactions in Organic Solvents. One objective of this research was to provide a predictive background for radical heterolysis reactions that give unsubstituted alkene radical cations in typical organic solvents. Correlations of the rate constants for heterolysis of radicals **5** with solvent polarity provide the most important information in that regard. The magnitudes of the solvent effects on the rates of these reactions were similar to those found for radical heterolysis reactions that give styrene and enol ether radical cations, and it seems likely that solvent effects for radicals lacking the reporter group moiety also will be similar.

For a working model, we assume that the correlations shown in Figure 5 will apply for simple β-(ester)alkyl radicals; that is, that rate constants will correlate with $E_T(30)$ values with slopes of 0.115. The limit for the rate constant for heterolysis of mesylate radical **4a** in acetonitrile ($k_{het} > 5 \times 10^9$ s^{-1}) and the rate constant for heterolysis of phosphate radical **4b** in acetonitrile ($k_{het} = 4 \times 10^6$ s^{-1}) provide anchor points on a kinetic scale for these types of alkyl radicals. The average ratio of rate constants for reaction of radicals **5a** and **5b** in the common solvents studied was 5; therefore, we assume that β-trifluoroacetate alkyl radicals will react 0.2 times as fast as β-diphenyl phosphate alkyl radicals, or $k_{het} = 8 \times 10^5$ s^{-1} in CH_3CN. The kinetic values are collected in Figure 7, which provides estimates for the rate constants for heterolysis reactions of the various radicals at ambient temperature as a function of solvent polarity on the $E_T(30)$ scale.[17]

(38) Bales, B. C.; Horner, J. H.; Huang, X. H.; Newcomb, M.; Crich, D.; Greenberg, M. M. *J. Am. Chem. Soc.* **2001**, *123*, 3623−3629.
(39) Brown, H. C.; Peters, E. N. *J. Am. Chem. Soc.* **1977**, *99*, 1712−1716.
(40) Kirmse, W.; Krzossa, B.; Steenken, S. *J. Am. Chem. Soc.* **1996**, *118*, 7473−7477.
(41) Whitted, P. O.; Horner, J. H.; Newcomb, M.; Huang, X. H.; Crich, D. *Org. Lett.* **1999**, *1*, 153−156.

Scheme 7

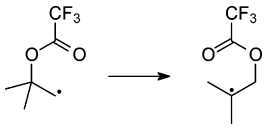

The predictions in Figure 7 appear to be reasonable. For example, Ingold and co-workers studied the rearrangement of the β-trifluoroacetoxy radical shown in Scheme 7.[42] The rate constant for rearrangement in $CF_2ClCFCl_2$ at 75 °C obtained by kinetic ESR spectroscopy was $k = 7 \times 10^4$ s^{-1}. Using a log A term of 11.2 and adjusting for the fact that the method typically gave rate constants that were too small by a factor of 2, the estimated rate constant for the rearrangement at 20 °C would be $k \approx 1 \times 10^4$ s^{-1}. From Figure 7, the predicted rate constant for heterolysis of β-trifluoroacetoxy radicals that give trisubstituted alkene radical cations in $CF_2ClCFCl_2$, $E_T(30) = 33.2$,[17] at 20 °C is $k \approx 3 \times 10^4$ s^{-1}. It would appear that the rearrangement in Scheme 7 proceeds by initial heterolysis and ion pair recombination.

The estimated rate constants in Figure 7 can be used in combination with known rate constants for radical trapping reactions to predict the relative amounts of radical trapping and heterolysis that would be expected in a typical radical chain reaction. β-Mesylate radicals heterolyze so rapidly that they should fragment faster than H-atom trapping by tin hydride even in a low polarity solvent such as benzene, and they are an obvious choice if one wishes to generate an alkene radical cation for an intermolecular reaction. β-Trifluoroacetate radicals in benzene, on the other hand, would be largely reduced by tin hydride ($k_H = 2 \times 10^6$ M^{-1} s^{-1})[43] at 0.1 M concentration.

In addition to the predicted rate constants at ambient temperature for heterolytic fragmentations, one can estimate temperature effects on these reactions. The log A values for heterolysis of radical **5a** found here for reactions in THF and acetonitrile (log $A = 11.2$) are quite similar to those found in other radical heterolysis reactions that gave styrene radical cations and enol ether radical cations,[18−20,30] and it seems reasonable to assume that this entropic term will be approximately correct for most radical heterolysis reactions. The log A value reflects net entropy demand in the fragmentation transition state,[44] but intermolecular reactions typically have larger negative entropies of activation, resulting in log A terms of ca. 9. The result is that bimolecular reactions will be less sensitive to temperature effects than the heterolysis reactions.

One important point is that the rate constants for heterolytic fragmentation are not equivalent to the rate constants for formation of diffusively free radical cations. In the case of an isomerization reaction or an intramolecular nucleophilic capture reaction, the radical cation might react in the CIP, but intermolecular capture is limited by diffusional processes and cannot compete with CIP collapse. CIP partitioning between collapse to the starting radical or its isomer and diffusive escape will be controlled largely by the stability of the ions and the solvent polarity. For the CIP produced from β-mesylate radical **4a**, CIP collapse in acetonitrile was slower than heterolytic fragmentation of the radical, and the CIP is favored at equilibrium. The rate constants at ambient temperature for diffusive escape from various CIPs in acetonitrile are in the range of $(2-30) \times 10^8$ s^{-1},[8,20,31] and these rate constants, combined with the favorable equilibrium for CIP formation, will result in large concentrations of diffusively free ions. Collapse of the CIP produced from β-phosphate radical **4b** in acetonitrile was estimated to have a rate constant on the order of $k_{rec} = 1 \times 10^9$ s^{-1}, however. This collapse rate constant could be up to an order of magnitude faster than escape from the CIP in CH_3CN. CIP escape rate constants in solvents less polar than acetonitrile will be slower, and it is likely that effectively no diffusively free ions can form from β-phosphate radicals in low-polarity solvents.

Conclusion

Radical heterolysis reactions offer an attractive synthetic entry to radical cations, but little was known about the kinetics of radical heterolysis reactions that give simple alkene radical cations. The present work resulted in kinetic values that provide a foundation for understanding these reactions and might be used for designing synthetic conversions. An overriding theme is the remarkably low barriers for the charge-forming fragmentation reactions, even though the alkene radical cation products do not contain stabilizing aryl or ether groups. The β-mesylate radical heterolysis reaction in acetonitrile is faster than ion pair collapse, and this feature will result in the rapid accumulation of diffusively free radical cations. The β-phosphate radical heterolysis is a relatively fast process that should compete favorably with H-atom transfer in typical synthetic radical chain reaction applications. The estimated rate constants for radical heterolysis in various solvents shown in Figure 7 can be improved by detailed studies of specific radicals, but we believe they will provide useful starting points for synthetic planning purposes.

Experimental Section

The synthetic procedures for compounds used in this work are described in the Supporting Information.

Laser Flash Photolysis Studies. Acetonitrile (HPLC grade) used in LFP studies was purchased from Fisher Scientific and used as received. LFP studies were performed with Applied Photophysics LKS-50 and LKS-60 kinetic spectrometers using Nd:YAG lasers with irradiation at 355 nm. Solutions of the PTOC precursor having an absorbance of 0.2−0.5 AU at 355 nm were placed in a thermally jacketed addition funnel and sparged with a stream of helium for 15−30 min. The temperature of the solution was adjusted by circulation of a water/methanol solution from a regulated bath through the jacket. The solutions were allowed to flow through a quartz cell (1 cm × 1 cm i.d.). Temperatures were measured with a thin wire copper/constantan thermocouple placed in the flowing stream immediately above the irradiation region of the flow cell. For studies conducted below 10 °C, the addition funnel and flow cell were placed in a nitrogen-purged box fitted with quartz windows. For kinetic runs, several traces typically were averaged to improve signal-to-noise. Curve fitting of kinetic traces was achieved with Applied Photophysics software supplied with the spectrophotometers.

Photolysis of 1b in CD_3CN with Thiophenol. A stock solution of the PTOC ester (**1b**) was prepared in CD_3CN. A solution of thiophenol in CD_3CN (1 mL) contained in a 5 mm NMR tube or a 1-mL volumetric flask was deoxygenated for 2 min with a stream of nitrogen from a syringe needle inserted into the tube through a rubber septum cap. A stock solution of PTOC ester precursor in CD_3CN (100 or 200 μL)

(42) Barclay, L. R. C.; Lusztyk, J.; Ingold, K. U. *J. Am. Chem. Soc.* **1984**, *106*, 1793−1796.
(43) Chatgilialoglu, C.; Newcomb, M. *Adv. Organomet. Chem.* **1999**, *44*, 67−112.
(44) At ambient temperature, log $A = 13.1$ when $\Delta S^{\ddagger} = 0$.

was added, and nitrogen was passed through the solution for an additional minute. The initial thiophenol concentration ranged from 0.04 to 0.8 M, and the PTOC ester concentration was 0.02 M. The solutions were irradiated with a 150 W floodlamp for 15−20 min. The ratio of **10** to **11** was determined by ^{1}H NMR spectroscopy by integration of the signals for H-3 of **10** (δ 4.96) and of **11** (δ 5.13). The error in the integrals was estimated to be ±10% of the measured value, and errors in the ratios were determined by standard error propagation. In Figure 3, the [**10**]/[**11**] ratio was plotted against the average thiophenol concentration estimated as $[PhSH]_{average} = 0.5([PhSH]_{initial} + [PTOC]_{final})$. The results of the studies are listed in Table S2 in the Supporting Information.

Photolysis of 1a in CD_3CN with Thiophenol. The procedure was the same as that described above for **1b**. 2-Methyl-2-heptene (**11**) was the only product observed by NMR spectroscopy. Yields of **11** determined by GC (DB-5 column) with ethylbenzene as an internal standard were 61−76%.

Photolysis of 1a in Methanol with *tert*-Butyl Thiol. A solution (0.9 mL) of *tert*-butyl thiol (0.05 M) in methanol was deoxygenated for 3 min with a stream of nitrogen. A solution of **1a** (0.1 M, 100 uL) in CD_3CN was added. The solution was deoxygenated for a further 3 min and irradiated for 40 min with a 150 W flood lamp. A solution (9 mL) of ethylbenzene (0.128 mg/mL) in THF was added, and the resulting mixture was analyzed by gas chromatography (DB-5 column). Response factors were determined with authentic samples of the two ethers. Yields of 70% ± 3% and 20% ± 0.7% were obtained for 2-methoxy-2-methyl-2-heptane and 3-methoxy-2-methyl-2-heptane, respectively.

Acknowledgment. This work was supported by a grant from the National Science Foundation (CHE0235293).

Supporting Information Available: Synthetic methods, detailed kinetic results, and NMR spectra. This material is available free of charge via the Internet at http://pubs.acs.org.

JA046089G